Atomic Data and Nuclear Data Tables 102 (2015) 1–5

Contents lists available at ScienceDirect

Atomic Data and Nuclear Data Tables

journal homepage: www.elsevier.com/locate/adt

Copper fine-structure K-shell electron impact ionization cross sections for fast-electron diagnostic in laser-solid experiments

P. Palmeri [a,*], P. Quinet [a,b], D. Batani [c]

[a] Astrophysique et Spectroscopie, Université de Mons - UMONS, B-7000 Mons, Belgium
[b] IPNAS, Université de Liège, B-4000 Liège, Belgium
[c] CELIA, Université de Bordeaux 1, F-33400 Talence, France

ARTICLE INFO

Article history:
Received 26 August 2014
Received in revised form
1 December 2014
Accepted 1 December 2014
Available online 26 December 2014

Keywords:
Atomic processes
Electron impact ionization
Inner-shells
Hot plasmas
High densities
Relativistic effects

ABSTRACT

The K-shell electron impact ionization (EII) cross section, along with the K-shell fluorescence yield, is one of the key atomic parameters for fast-electron diagnostic in laser-solid experiments through the K-shell emission cross section. In addition, copper is a material that has been often used in those experiments because it has a maximum total K-shell emission yield. Furthermore, in a campaign dedicated to the modeling of the K lines of astrophysical interest (Palmeri et al., 2012), the K-shell fluorescence yields for the K-vacancy fine-structure atomic levels of all the copper isonuclear ions have been calculated.

In this study, the K-shell EII cross sections connecting the ground and the metastable levels of the parent copper ions to the daughter ions K-vacancy levels considered in Palmeri et al. (2012) have been determined. The relativistic distorted-wave (DW) approximation implemented in the FAC atomic code has been used for the incident electron kinetic energies up to 10 times the K-shell threshold energies. Moreover, the resulting DW cross sections have been extrapolated at higher energies using the asymptotic form proposed by Davies et al. (2013).

© 2014 Elsevier Inc. All rights reserved.

* Corresponding author.
E-mail addresses: patrick.palmeri@umons.ac.be (P. Palmeri), pascal.quinet@umons.ac.be (P. Quinet), batani@celia.u-bordeaux1.fr (D. Batani).

http://dx.doi.org/10.1016/j.adt.2014.12.001
0092-640X/© 2014 Elsevier Inc. All rights reserved.

Contents

1. Introduction 2
2. Calculations 2
3. Summary and conclusion 4
Acknowledgment 4
Appendix A. Supplementary data 4
References 4
Explanation of Tables 5
Table 1. Fine-Structure Energy Levels in the Copper Isonuclear Sequence, from Cu^0 to Cu^{27+} 5
Table 2. Parameters for the Fine-Structure K-shell EII Cross Sections in the Copper Isonuclear Sequence, from Cu^0 to Cu^{27+} 5

1. Introduction

The K-shell electron impact ionization (EII) cross section, along with the K-shell fluorescence yield, is one of the key atomic parameters for fast-electron diagnostic in laser-solid experiments through the K-shell emission cross section [1]. The study of fast electrons generated in these experiments is of interest, for instance, in shock [2] and fast [3] ignitions in inertial confinement fusion (ICF) and in energetic secondary particle production [4]. The Kα emission generated by the EII process is analyzed by either imagers which provide spatial and temporal information of relativistic electrons [5] or spectrometers which provide bulk electron temperatures [6]. In addition, copper is a material that has been often used in those experiments because it has a maximum total K-shell emission yield [1].

During a campaign dedicated to the modeling of the K lines of astrophysical interest, the K-shell fluorescence yields for the K-vacancy fine-structure atomic levels of all the copper isonuclear ions have been calculated along with other fundamental decay parameters [7]. Moreover, the fine-structure effects on the iron K line shape with diagnostics implications have been studied in details for astrophysical photoionized plasmas where the dominant process that populates K-vacancy levels is photoionization [8].

The purpose of this work is to provide the missing fine-structure K-shell EII cross sections required for modeling the Cu K lines produced in laser-solid experiments and that complement the decay data of Palmeri et al. [7] in order to take advantage of potential diagnostics of a fine-structure description.

2. Calculations

The Flexible Atomic Code (FAC) [9] has been used to compute the EII cross sections by the relativistic distorted-wave (DW) method. In this method, the total EII cross section $\sigma_{ij}^{EII}(\varepsilon)$ (in atomic unit) from the initial fine-structure state ψ_i to the final ionized fine-structure state ψ_j at the incident electron kinetic energy ε is expressed in terms of the EII collision strength

$$\sigma_{ij}^{EII}(\varepsilon) = \frac{1}{k^2(2J_i+1)} \int_0^{\frac{\varepsilon - I_{ij}}{2}} \Omega_{ij}^{EII}(\varepsilon, \varepsilon')\, d\varepsilon' \tag{1}$$

$$\Omega_{ij}^{EII} = 2 \sum_{\kappa_i \kappa_j \kappa} \sum_{JJ_T} (2J_T+1) \times \left| \langle \psi_i\, \kappa_i, J_T M_T | \sum_{n<m} \frac{1}{r_{nm}} | (\psi_j\, \kappa) J\, \kappa_j, J_T M_T \rangle \right|^2 \tag{2}$$

where k is the incident electron kinetic momentum, J_i the total angular momentum of the target state ψ_i, ε' the kinetic energy of the scattered electron, I_{ij} the threshold energy of the fine-structure transition $\psi_i \rightarrow \psi_j$, κ_i, κ_j, and κ the relativistic angular quantum numbers of respectively the incident, the scattered and the ejected electrons, J the total angular momentum resulting from the coupling of the final ionized state ψ_j and the ejected electron momentum κ, J_T the total angular momentum resulting from the coupling of J and the scattered electron momentum κ_j which must be equal to the coupling of the initial state ψ_i with the incident electron momentum κ_i, M_T the corresponding projection of J_T, i.e. the total magnetic quantum number. In addition, energy conservation imposes $\varepsilon = I_{ij} + \varepsilon' + \varepsilon''$ where ε'' is the kinetic energy of the ejected electron.

The N electron atomic state functions (ASF) $|\psi\rangle$ are superpositions of configuration state functions (CSF) $|\phi_v\rangle$ of the same conserved symmetries, i.e. parity, total angular momentum J_T and its projection M_T

$$|\psi\rangle = \sum_v a_v\, |\phi_v\rangle \tag{3}$$

where a_v are mixing coefficients determined by solving the secular equation of the N electron Dirac–Coulomb–Breit Hamiltonian.

The CSFs are antisymmetric sums of products of N one-electron Dirac spinors

$$\varphi_{n\kappa m} = \frac{1}{r} \begin{pmatrix} P_{n\kappa}(r)\ \chi_{\kappa m}(\theta, \phi, \sigma) \\ iQ_{n\kappa}(r)\ \chi_{-\kappa m}(\theta, \phi, \sigma) \end{pmatrix} \tag{4}$$

where the radial functions $P_{n\kappa}$ and $Q_{n\kappa}$ are respectively the large and small components and $\chi_{\kappa m}$ is the usual spin-angular function. n is the principal quantum number and κ is the relativistic angular quantum number which is related to the orbital l and the total angular momentum j of the electron through $\kappa = (l-j)(2j+1)$ where m is its magnetic quantum number. The radial functions are solutions of the Dirac–Fock–Slater (DFS) equations for the bound electrons where the local central potential is constructed using a fictitious mean configuration with fractional occupation numbers determined from the set of CSFs used to build the ASFs. The free electron radial functions are distorted-waves determined by solving the DFS equations using the same local central potential as for the bound orbitals.

In the present study, the target ASFs were built considering the same lists of configurations as in Ref. [7]. As the transition operator used in Eq. (2) is the Coulomb interaction operator, the high-energy rise of the EII cross section due to the Breit interaction (see e.g. Ref. [10]) will therefore not be taken into account by our FAC calculations. This relativistic rise starts at incident electron kinetic energy $\varepsilon \sim 100$ keV [11]. In order to consider this effect but also the density effect, the empirical trend proposed by Davies et al. [1] (Eq. (B3) of this reference) for Cu^0 is used to extrapolate our fine-structure DW EII cross sections to incident electron kinetic energies greater than 100 keV.

The resulting EII cross sections are expressed in barn using the following parametrized formula for each fine-structure transition $\psi_i \rightarrow \psi_j$

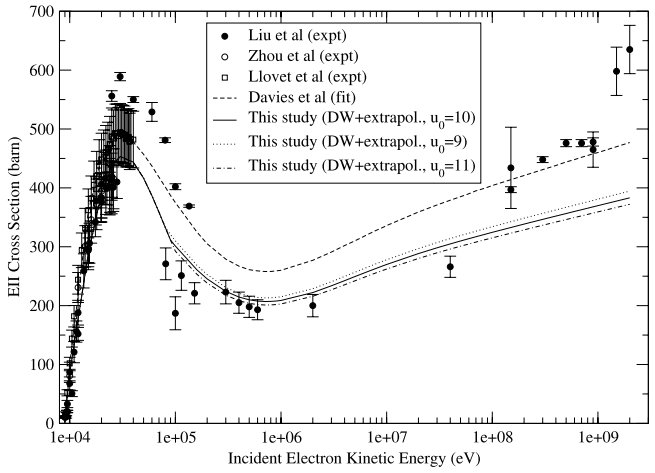

Fig. 1. Comparison of the DW + extrapol K-shell EII cross sections with experiment and the empirical fit of Davies et al. [1] in Cu^0. Solid line: DW + extrapol with an overpotential limit $u_0 = 10$; dot line: DW + extrapol with an overpotential limit $u_0 = 9$; dot–dash line: DW + extrapol with an overpotential limit $u_0 = 11$; dash line: empirical fit by Davies et al. [1]; full circles: compilation of experimental data by Liu et al. [13]; open circles: measurements by Zhou et al. [14]; open squares: measurements by Llovet et al. [15].

$$\sigma_{ij}^{EII}(u) = \frac{3.80998406E+08}{(2J_i+1)\,u\,I_{ij}} \times \left\{ A_{ij}\,ln(u) + B_{ij}\left(1-\frac{1}{u}\right)^2 + \left(\frac{C_{ij}}{u}+\frac{D_{ij}}{u^2}\right)\left(1-\frac{1}{u}\right)\right\} \quad \text{for } u \le u_0 = 10$$

$$= K_{ij} \times 20.95 \times \left(1-\frac{0.2824}{u}\right)\left(1-\frac{1}{\left(\frac{u\,I_{ij}}{0.511E+06}+1\right)^2}\right)^{-1} \times \ln\left[\left(\frac{u+113.8}{114.8}\right)^{1/2}\frac{57.0098\,u}{56.9+0.1098\,u}\right] \quad \text{for } u > u_0 = 10 \tag{5}$$

where $u = \varepsilon/I_{ij}$ is the overpotential, A_{ij}, B_{ij}, C_{ij}, and D_{ij} are dimensionless coefficients fitted to the corresponding fine-structure DW cross sections calculated for $u \le 10$. The formula used for $u \le 10$ is the one given by Fontes et al. [12]. The extrapolation coefficient K_{ij} is the ratio between $\sigma_{ij}^{EII}(u = 10)$ and the K-shell emission cross section evaluated at $u = 10$ given by Eq. (B3) in Ref. [1] used here for $u > 10$. In copper ions where 8.9 keV $\le I_{ij} \le$ 10.9 keV (see Table 2, Appendix A), an overpotential limit of $u_0 = 10$ corresponds to a kinetic energy limit of $\varepsilon_0 \sim 100$ keV where the Breit interaction effect becomes important. In Table 1 (see Appendix A), the 9628 copper ion fine-structure energy levels calculated by Palmeri et al. [7] to evaluate their decay properties and considered here for the K-shell EII process are listed. Table 2 contains the K-shell EII cross section parameters used in Eq. (5) for the 35,793 fine-structure K-shell transitions between the levels reported in Table 1 (see Appendix A).

In Fig. 1, our calculated K-shell EII cross sections in Cu^0 are compared to the experimental data compiled by Liu et al. [13], the measurements of Zhou et al. [14] and of Llovet et al. [15] and the fitted cross section of Davies et al. [1]. Our DW + extrapol. cross section curves are summations over all the fine-structure transitions from the Cu^0 ground level. The measurements of Llovet et al. [15] are systematically higher than our calculations although our curves cross their 10% error bars for most of their experimental values. The agreement with Zhou et al. [14] and with the low-energy data ($\varepsilon \le 150$ MeV) of Liu et al. [13] (with the exception of the measurements of Davis et al. [16]) is reasonably good (better than 2 error bars for most of the experimental points). The experimental cross sections of Davis et al. [16] (25 keV $\le \varepsilon \le$ 80 keV) seems too high and their few-percents error bars may be underestimated. The high-energy measurements ($\varepsilon > 150$ MeV) of Middleman et al. [17], Ishii et al. [18] and Genz et al. [19] compiled by Liu et al. [13] disagree with the high energy trend of our calculations. A 10% change on the overpotential limit u_0 alters our high-energy DW + extrapol cross sections by a few percents as shown in this figure. The fitted cross sections of Davies et al. [1] are systematically ~10%–~20% higher than our calculations.

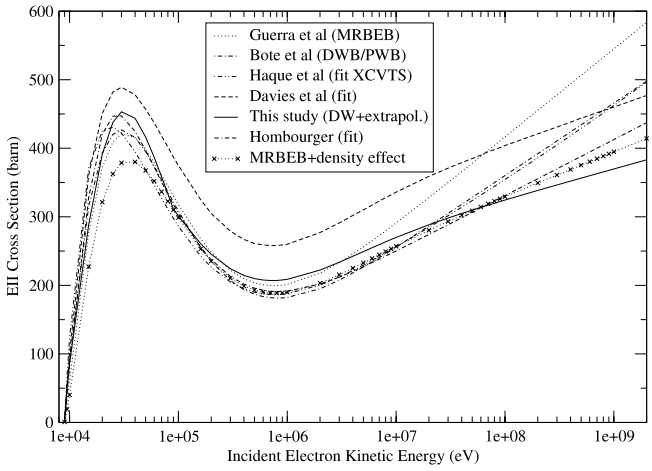

Fig. 2. Comparison of the DW + extrapol K-shell EII cross section with other models in Cu^0. Solid line: DW + extrapol; dashed line: empirical fit of Davies et al. [1]; dot line: MRBEB [11]; dot–dash line: DWB/PWB [20]; double-dot–single-dash line: empirical XCVTS fit [21]; single-dot–double-dash line: empirical fit of Hombourger [22]; dot line with crosses: MRBEB model [11] corrected for density effect as suggested by Davies et al. [1].

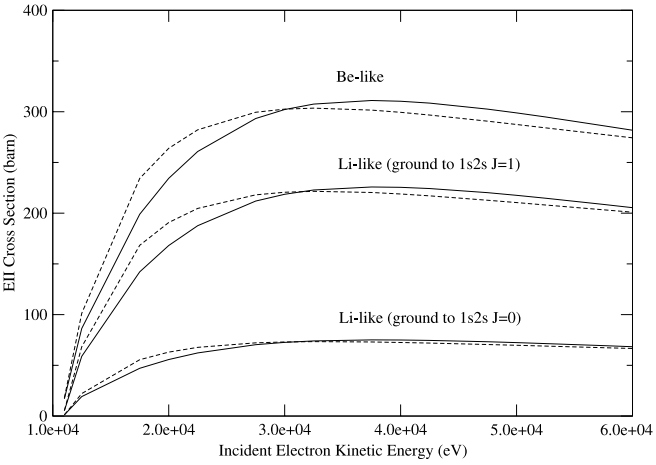

Fig. 3. Comparison of the K-shell EII cross sections in Li-like ($N = 3$) and Be-like ($N = 4$) Cu. Solid lines: DW calculations (this work) where only the Coulomb interaction is considered for the scattering matrix (see Eq. (2)). Dash lines: DW calculations of Fontes et al. [10] where the Breit interaction is taken into account. The Be-like curves are sums over all the fine-structure contributions from the ground level.

A comparison of our (summed) DW + extrapol cross section in Cu^0 with other models [1,11,20–22] is given in Fig. 2. From threshold to the dip, our cross section is closed to the *ab initio* models presented, i.e. the modified relativistic binary encounter Bethe (MRBEB) model of Guerra et al. [11] and the combination of

distorted-wave-Born and plane-wave-Born (DWB/PWB) models of Bote et al. [20]. A good agreement is also observed for the empirical models of Haque et al. [21] and Hombourger [22]. Beyond the dip ($\varepsilon > 10$ MeV), the relativistic rise is steeper than in our model in both *ab initio* calculations (MRBEB and DWB/PWB) as well as in the fitted cross sections of Haque et al. [21] and Hombourger [22]. Following the suggestion of Davies et al. [1], the density-effect correction has been incorporated into the MRBEB model and the result is plotted in this figure. This last model (MRBEB+density effect) shows the decrease of the relativistic rise compared to the MRBEB calculation due to the high density in the copper foil bringing the corrected MRBEB cross section closer to our DW + extrapol model. It can be also noticed that this correction lowers the peak by ∼10%.

In Fig. 3, our DW K-shell EII cross sections are compared in Li-like ($N = 3$) and Be-like ($N = 4$) copper with the DW fitted model of Fontes et al. [10] that takes into account the Breit interaction. The incident electron kinetic energy has been limited to 60 keV, i.e. $u \sim 6$, as suggested by Fontes et al. [10] as their fitted formulae are not expected to be reliable beyond that energy limit due to convergence problems in their DW calculations. The Be-like curves are sums over all the fine-structure contributions from the ground level. The agreements between our 'Coulomb only' model and the Coulomb–Breit model of Fontes et al. [10] are better than ∼20%. One can also notice the factor ∼4 difference between the fine-structure EII transitions $e^- + 1s^2 2s^2 S_{1/2} \rightarrow 1s2s^1\ S_0 + 2e^-$ and $e^- + 1s^2 2s^2 S_{1/2} \rightarrow 1s2s^3 S_1 + 2e^-$.

3. Summary and conclusion

The K-shell EII cross sections have been calculated for 35,793 fine-structure transitions along the copper isonuclear sequence from Cu^0 up to Cu^{27+}. The DW method as implemented in the FAC atomic code [9] has been used for overpotential of the incident electron up to $u = 10$. For $u > 10$, the cross sections have been extrapolated using the trend of the Cu^0 K-shell emission cross section recommended by Davies et al. [1]. The latter takes into account both the Breit interaction causing the high-energy relativistic rise as well as the density effect. These new ionization data in combination with the decay rates calculated by Palmeri et al. [7] should help to model the emissivities of the Cu K lines produced by fast-electron impacts in laser-solid experiments [23].

Acknowledgment

Financial support from the belgian FRS-FNRS is acknowledged. P.P. and P.Q. are respectively Research Associate and Research Director of this organization.

Appendix A. Supplementary data

Supplementary material related to this article can be found online at http://dx.doi.org/10.1016/j.adt.2014.12.001.

References

[1] J.R. Davies, R. Betti, P.M. Nilson, A.A. Solodov, Phys. Plasmas 20 (2013) 083118.
[2] S. Gus'kov, X. Ribeyre, M. Touati, J.L. Feugeas, Ph. Nicolaï, V. Tikhonchuk, Phys. Rev. Lett. 109 (2012) 255004.
[3] M. Tabak, J. Hammer, M.E. Glinsky, W.L. Kruer, S.C. Wilks, J. Woodworth, E.M. Campbell, M.D. Perry, R.J. Mason, Phys. Plasmas 1 (1994) 1626.
[4] J.T. Mendonça, J.R. Davies, M. Eloy, Meas. Sci. Technol. 12 (2001) 1801.
[5] P.M. Nilson, J.R. Davies, W. Theobald, P.A. Jaanimagi, C. Mileham, R.K. Jungquist, C. Stoeckl, I.A. Begishev, A.A. Solodov, J.F. Myatt, J.D. Zuegel, T.C. Sangster, R. Betti, D.D. Meyerhofer, Phys. Rev. Lett. 108 (2012) 085002.
[6] W. Theobald, K. Akli, R. Clarke, J.A. Delettrez, R.R. Freeman, S. Glenzer, J. Green, G. Gregori, R. Heathcote, N. Izumi, J.A. King, J.A. Koch, J. Kuba, K. Lancaster, A.J. MacKinnon, M. Key, C. Mileham, J. Myatt, D. Neely, P.A. Norreys, H.-S. Park, J. Pasley, P. Patel, S.P. Regan, H. Sawada, R. Shepherd, R. Snavely, R.B. Stephens, C. Stoeckl, M. Storm, B. Zhang, T.C. Sangster, Phys. Plasmas 13 (2006) 043102.
[7] P. Palmeri, P. Quinet, C. Mendoza, M.A. Bautista, J. García, M.C. Witthoeft, T.R. Kallman, Astronom. Astrophys. 543 (2012) A44.
[8] T.R. Kallman, P. Palmeri, M.A. Bautista, C. Mendoza, J.H. Korlik, Astrophys. J. Suppl. Ser. 155 (2004) 675.
[9] M.F. Gu, Astrophys. J. 582 (2003) 1241.
[10] C.J. Fontes, D.H. Sampson, H.L. Zhang, Phys. Rev. A 59 (1999) 1329.
[11] M. Guerra, F. Parente, P. Indelicato, J.P. Santos, Int. J. Mass Spectrom. 313 (2012) 1.
[12] C.J. Fontes, D.H. Sampson, H.L. Zhang, Phys. Rev. A 48 (1993) 1975.
[13] M. Liu, Z. An, C. Tang, Z. Luo, X. Peng, X. Long, At. Data Nucl. Data Tables 76 (2000) 213.
[14] C.G. Zhou, Z. An, Z.M. Luo, Chin. Phys. Lett. 18 (2001) 759.
[15] X. Llovet, C. Merlet, F. Salvat, J. Phys. B 33 (2000) 3761.
[16] D.V. Davis, V.D. Mistry, C.A. Quarles, Phys. Lett. 38A (1972) 169.
[17] L.M. Middleman, R.L. Ford, R. Hofstadter, Phys. Rev. A 2 (1970) 1429.
[18] K. Ishii, M. Kamiya, K. Sera, S. Morita, H. Tawara, M. Oyamada, T.C. Chu, Phys. Rev. A 15 (1977) 906.
[19] H. Genz, C. Brendel, P. Eschwey, U. Kuhn, W. Low, A. Richter, P. Seserko, Z. Phys. 305 (1982) 9.
[20] D. Bote, F. Salvat, A. Jablonski, C.J. Powell, At. Data Nucl. Data Tables 95 (2009) 871.
[21] A.K.F. Haque, M.R. Talukder, M. Shahjahan, M.A. Uddin, A.K. Basak, B.C. Saha, J. Phys. B 43 (2010) 115201.
[22] C. Hombourger, J. Phys. B 31 (1998) 3693.
[23] H.-K. Chung, M.H. Chen, R.W. Lee, High Energy Density Phys. 3 (2007) 57.

Explanation of Tables

Table 1. **Fine-Structure Energy Levels in the Copper Isonuclear Sequence, from Cu^0 to Cu^{27+}**

The fine-structure energy levels of Cu^0–Cu^{27+} considered in the K-shell EII cross sections presented in Table 2. This table is based on Table 9 of Ref. [7]. The configuration assignments and energies shown are those calculated by Palmeri et al. [7] using the HFR method. This is a sample of the table where only the data for $N = 2 - 4$ are given. The complete table is provided as a supplementary MS-Excell file.

N	The number of electrons of the copper ion
i	The fine-structure level index
$2S + 1$	The level multiplicity
L	The level total orbital angular momentum quantum number
$2J$	Two times the level total angular momentum quantum number
Configuration	The level configuration assignment
E (eV)	The level energy in eV

Table 2. **Parameters for the Fine-Structure K-shell EII Cross Sections in the Copper Isonuclear Sequence, from Cu^0 to Cu^{27+}**

This table presents the parameters used in Eq. (5) for each fine-structure K-shell transition $i \rightarrow j$ between the parent (N) and daughter (N') copper ions. This is a sample of the table where only the data for $N = 3 - 4$ are given. The complete table is provided as a supplementary MS-Excell file.

N	The number of electrons of the parent copper ion (see Table 1)
i	The parent ion level index (see Table 1)
N'	The number of electrons of the daughter copper ion (see Table 1)
j	The daughter ion level index (see Table 1)
$2J_i + 1$	The statistical weight of the parent ion level i
I_{ij} (eV)	The threshold energy for the fine-structure transition $i \rightarrow j$ (in eV)
A_{ij}	The A_{ij} coefficient of Eq. (5)
B_{ij}	The B_{ij} coefficient of Eq. (5)
C_{ij}	The C_{ij} coefficient of Eq. (5)
D_{ij}	The D_{ij} coefficient of Eq. (5)
K_{ij}	The extrapolation coefficient K_{ij} of Eq. (5)